# Stabilization of ablative Rayleigh-Taylor instability due to change of the Atwood number

Wenhua Ye,[1,2,*] Weiyan Zhang,[2] and X. T. He[1,2]
[1]*Department of Physics, Zhejiang University, Hangzhou 310028, People's Republic of China*
[2]*Institute of Applied Physics and Computational Mathematics, P.O. Box 8009, Beijing 100088, People's Republic of China*
(Received 29 March 2001; revised manuscript received 1 November 2001; published 21 May 2002)

Recent experiment [S.G. Glendinning *et al.*, Phys. Rev. Lett. **78**, 3318 (1997)] showed that the measured growth rate of laser ablative Rayleigh-Taylor (RT) instability with preheating is about 50% of the classic value and is reduced by about 18% compared with the simulated value obtained with the computer code LASNEX. By changing the temperature variation of the electron thermal conductivity at low temperatures, the density profile from the Bhatnagar-Gross-Krook approximation is recovered in the simulation, and the simulated RT growth rate is in good agreement with the experimental value from Glendinning *et al.* The preheated density profile on ablative RT stablization is studied numerically. A change of the Atwood number in the preheating case also leads to RT stabilization. The RT growth formula $\gamma=\sqrt{Akg/(1+AkL)}-2kV_a$ agrees well with experiment and simulation, and is appropriate for the preheating case.

DOI: 10.1103/PhysRevE.65.057401 PACS number(s): 52.35.Py, 81.15.Fg

Hydrodynamic instability places a fundamental limit on design parameters required for a capsule ignition of the inertial confinement fusion (ICF) [1]. In an ICF capsule implosion, the ablation front is Rayleigh-Taylor (RT) unstable. An accurate prediction of the RT growth is essential to the design of the ignition capsule, particularly for directly driven ICF [2]. The Takabe formula $\gamma_T=0.9\sqrt{kg}-\beta kV_a$ [3], which includes the ablation advection stabilization, is frequently used to discuss the linear growth rate of laser ablative RT instability, where $k$ is the perturbed wave number, g is the acceleration, $V_a$ is the ablation velocity, and $\beta\simeq 3\sim 4$ is expected in the direct-drive ablation. A modified version of the Takabe formula, which includes stabilization of the ablation advection and the density gradient scale length, was given by Lindl as $\gamma_{mT}=\sqrt{kg/(1+kL)}-\beta kV_a$ [1], where $L=[\rho/(d\rho/dz)]_{min}$ is the density gradient scale length and $\beta=2$ was given, for example, by Sanz [4]. In this paper we refer to this formula as the modified-by-Lindl Takabe formula or the Lindl formula. However, the reduction in growth of laser ablative RT instability in recent experiments [5–7], which deviates the modified-by-Lindl Takabe formula, is observed and has not fully been explained.

Recent experiments [5,6] have indicated that the growth rate of the areal density perturbation is significantly reduced as compared with the calculated results of the Spitzer-Harm (SH) electron thermal conductivity [8]. Glendinning *et al.* (GL) recognized that the difference between the experiment and the LASNEX simulation is due to a change in the longitudinal density profile resulting from preheating by energetic electrons. Honda *et al.* (HM) [9] calculated the lower RT growth rate using the two-dimensional (2D) full Fokker-Planck (FP) equation to compare with the SH electron transport coefficient, and showed that the density of the ablation front is changed from 2.0–2.4 g/cm$^3$ for SH and to 1.5–1.7 g/cm$^3$ for FP. GL simulated the foil acceleration in 1D geometry using the Bhatnagar-Gross-Krook (BGK) approximation [10] to the FP equation, and obtained a density distribution similar to the FP results given by HM. We do 2D simulations to further discuss the experiment result shown by GL. A similar change in the density profile is also seen by enhancing the electron thermal conductivity at low temperatures, and the RT growth rate in our simulation is in agreement with the GL's experimental value. It is found that there is a greater than 10% discrepancy in RT growth rate between our simulation and the modified-by-Lindl Takabe formula. We notice that this also occurs in Figs. 5 and 6 of Ref. [5]. Similarly, the FP result from HM was somewhat lower than the prediction of the modified-by-Lindl Takabe formula, using the BGK parameters. There may exist some physical reason that is not widely known. We see from the simulated density profile that the peak density of the ablation front drops considerably, so the Atwood number of the ablation front clearly decreases. Preheating not only enhances the stabilizations by the ablative advection and the finite density gradient scale length, but also leads to stabilization by the decreased Atwood number. The latter is another possible source for the reduction of ablative RT growth rates in the preheating case. Most of the heuristic formulas neglect the Atwood number because it takes a value of order unity in the less preheating case. Betti *et al.* gave a heuristic form $\gamma_{mL}=\sqrt{Akg/(1+AkL)}-\beta kV_a$ [11], here referred to as the modified Lindl formula. We find that the prediction of this formula is in closer agreement with GL's experimental value [5] and all our simulations. Preheating the ablation front is a useful way to stabilize the RT instability. Through effective preheating to the ablation front by x ray, the ablative RT growth and the laser imprint are suppressed in recent experiments [12,13]. In some designs of the National Ignition Facility (NIF) capsule, the RT stabilization by preheating of the shock, x ray etc., is important [14], so stabilization by decreased Atwood number can be a primary stabilization source.

The finite difference radiation hydrodynamic code LARED-S [15] is used in numerical simulations. LARED-S deals with compressible hydrodynamics, nonlinear electron conduction, multigroup radiation diffusion, ray tracing of laser absorbed by the inverse bremsstrahlung. The hydrodynamic equations

*Email address: Ye_wenhua@mail.iapcm.ac.cn

 

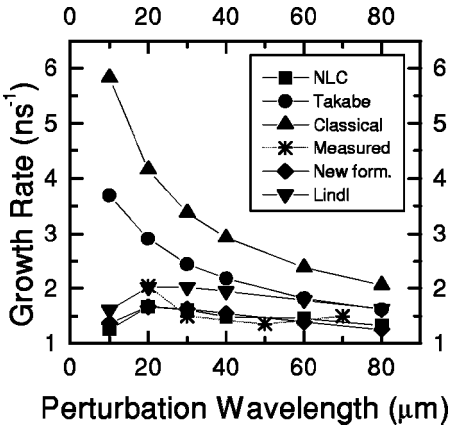


FIG. 1. Comparison of ablative growth rates for different formulas, the experiment and simulations for the 20-$\mu$m CH foil.

are integrated with the flux-corrected transport (FCT) algorithm [16] in space and the second-order Runge-Kutta method in time. The FCT with sixth-order accurate phase error is used and has second-order accuracy on the uniform part of the grid. The LARED-S code uses the slide zone version of FCT to trace the ablation surface and the fine uniform grids cluster near the steep ablation front. Simulations of the ablative RT instability in this paper are in two-dimensional Cartesian geometry.

The linear RT growth rate of the 2D simulation comes from the exponential fit of the Fourier amplitude of the areal density perturbation in the linear stage. The foil acceleration, the ablative velocity, the Atwood number, and the density gradient scale length are obtained by the parabolic fit to the one-dimensional simulation results during the same period. The Atwood number $A$ is $(\rho_2-\rho_1)/(\rho_2+\rho_1)$, where $\rho_2$ is chosen as $\rho_a$, the peak density at the ablation front, and as in Ref. [17], $\rho_1$ is the blow-off density, located at $(2k)^{-1}$ from the position of peak density. The ablative RT growth experiment performed by GL under conditions of a 20-$\mu$m-thin CH foil, a drive laser pulse with a linear 1-ns ramp to a peak intensity $7\times10^{13}$ W/cm$^2$ at the wavelength 0.53 $\mu$m, followed by a 2-ns flat section.

In our simulation, the electron thermal conductivity is considered in the form $\kappa=\kappa_{SH}f(T)h$, where $\kappa_{SH}\propto T^{5/2}$ is the SH formula and $T$ is the electron temperature. $h$ has a simple form of $1/[1+B\ln(T_{max}/T_0)]$ and is due to the fact that there exists a large temperature gradient near the critical surface, and the static potential effect has to be considered in electron thermal conduction [18], where $T_{max}$ is the maximum electron temperature in the corona region, $T_0$ is the electron temperature at the critical surface, and $B$ is an adjustable parameter, usually $B=1$. It was found that the electron thermal conductivity scales as 1/k at large $k$ when there exists a nonnegligible electrostatic field, where $k=\ln(T_{max}/T_0)$. A function $f(T)$ is due to the preheating effect of energetic electrons, which is considered in a form of $f(T)=a$ when $T>43$ eV and $f(T)=b/T+c/T^{3/2}$ when 1 eV$<T\leqslant43$ eV to meet the experiment result of GL, where $a$, $b$, $c$ are adjustable parameters. $f(T)$ is adjusted so that the density profile around the ablation front is close to the numerical solution for the 1D BGK [5] or for the FP equation of electron thermal transport [9,19], and it could be explained that the preheated ablation produces a lower temperature tongue at the head of the sharp front that is due to the SH electron thermal conduction. The tongue seems to be from an energetic electron contribution because energetic electrons have a longer mean free path.

The SH formula is rigorously valid only for fully ionized nondegenerate plasmas, i.e, for lower density and higher temperature. The application of the SH formula to dense plasmas can give erroneous results. The electron thermal conductivity calculated from the SH formula at a solid density and low temperature $T<10$ eV is incorrect by a large factor, which was shown by Tabak *et al.* [20]. The work of Lee and More gave some support to the arbitary change of the temperature variation of the electron thermal conductivity at lower temperatures [21]. The FP simulation showed that preheating by the electrons in the tail of the Maxwellian distribution is important for the density profile, and so more energy is transferred to the ablation front for FP than for SH. Our simulation shows that the density profile around the ablation front is very sensitive to the electron thermal conductivity at the head of the ablation front. In order to obtain the ablative RT growth rate in agreement with the experiment, it is possible to find a function $f(T)$ to fit the FP or the BGK density profile in the hydrodynamic simulation.

For $f(T)=1$, the ablation front is sharp due to less preheating, thus the linear RT growth rate from simulation agrees with the value of the Takabe formula. $f(T)$ is adjusted near the ablation front as follows:

$$f(T)=\begin{cases}1.0, & T<0.86\ \text{eV}\\ 10000, & 0.86\ \text{eV}\leqslant T<4.3\ \text{eV}\\ 4000, & 4.3\ \text{eV}\leqslant T<8.6\ \text{eV}\\ 1500, & 8.6\ \text{eV}\leqslant T<17.2\ \text{eV}\\ 300, & 17.2\ \text{eV}\leqslant T<43\ \text{eV}\\ 2.5, & 43\ \text{eV}\leqslant T<86\ \text{eV}\\ 1.5, & 86\ \text{eV}\leqslant T<172\ \text{eV}\\ 1.0, & T\geqslant172\ \text{eV},\end{cases}$$

which can be fit to $f(T)=186/T+11.5/T^{3/2}$ when 0.86 eV $<T<43$ eV, where $T$ is in units of 100 eV as used in the simulation code, so the electron thermal conductivity versus temperature is $T^{5/2}f(T)=11.5T+186T^{3/2}$, which produces a slowly varying temperature profile as in the BGK or in the FP simulation. The density profile is similar to the BGK result [5], and L is increased from 1 $\mu$m at $f(T)=1$ to about 4 $\mu$m at the above $f(T)$. As shown in Fig. 1, the linear growth rate of RT instability from our simulation, as seen in the curve "NLC," agrees well with the measured value by GL, as shown by the curve "measured," but is lower than the prediction from the modified Takabe formula $\gamma_{mT}=\sqrt{kg/(1+kL)}-2kV_a$ (the curve "Lindl"). The Takabe formula $\gamma_T=0.9\sqrt{kg}-3kV_a$ shows greater value than the measured value.

There exists a discrepancy of over 10% between the Lindl formula and GL's experiment or our simulation. In order to

TABLE I. Comparison of ablative RT growth rates in different preheating cases for the 40-$\mu$m perturbation wavelength.

| Model | L ($\mu$m) | $A$ | $g$ ($\mu$m/ns$^2$) | $V_a$ ($\mu$m/ns) | $\gamma_c$ (ns$^{-1}$) | $\gamma_{cal}$ (ns$^{-1}$) | $\gamma_{mL}$ (ns$^{-1}$) | $\gamma_{mT}$ (ns$^{-1}$) | $\frac{\gamma_{cal}}{\gamma_c}$ | $\lvert\frac{\gamma_{cal}-\gamma_{mL}}{\gamma_{cal}}\rvert$ | $\lvert\frac{\gamma_{cal}-\gamma_{mT}}{\gamma_{cal}}\rvert$ |
|---|---|---|---|---|---|---|---|---|---|---|---|
| Case 1 | 4.04 | 0.706 | 17.88 | 0.3540 | 1.676 | 1.082 | 1.059 | 1.200 | 0.646 | 0.021 | 0.109 |
| Case 2 | 0.96 | 0.974 | 21.25 | 0.3144 | 1.827 | 1.656 | 1.585 | 1.604 | 0.906 | 0.043 | 0.031 |
| Case 3 | 1.53 | 0.974 | 17.10 | 0.2703 | 1.639 | 1.365 | 1.371 | 1.387 | 0.833 | 0.004 | 0.016 |
| Case 4 | 2.78 | 0.757 | 19.16 | 0.3246 | 1.735 | 1.228 | 1.207 | 1.346 | 0.708 | 0.017 | 0.096 |
| Case 5 | 3.23 | 0.727 | 17.80 | 0.3540 | 1.672 | 1.125 | 1.107 | 1.249 | 0.673 | 0.016 | 0.110 |
| Case 6 | 2.27 | 0.625 | 17.58 | 0.4099 | 1.662 | 1.032 | 1.059 | 1.298 | 0.621 | 0.026 | 0.258 |

understand the difference, an exponential density profile around the ablation front is assumed, and the RT growth rate $\gamma=\sqrt{Akg/(1+AkL)}$ is obtained at the approximation of linearity, incompressibility, no viscosity, and no heat transfer. For consideration of ablative advection stabilization, the ablative RT growth rate should be in the form $\gamma_{mL}=\sqrt{Akg/(1+AkL)}-2kV_a$ with the variable Atwood number that depends on the preheated density profile. This modified Lindl formula, i.e., the curve ''new form,'' agrees very well with GL's experimental curve ''measured'' and our simulation with preheating. In the preheating case, the electron thermal flux at the head of the ablation front increases considerably, thus the temperature profile is not so steep that the power index of the electron thermal conductivity is much less than 5/2 in the SH model. This leads to the reduction of the peak density at the ablation front, so the density profile becomes smooth to compare with the SH model. As a result, we find that the modified Lindl formula with variable Atwood number may predict the preheating case. Rigorous simulation for preheating by energetic electrons or x rays is complicated, so $f(T)$ is changed to study the preheating effect on ablative RT growth, especially the Atwood number effect.

Since we see from the above discussion that a thin CH foil with 20 $\mu$m thickness is used in GL's experiment, the thin target easily expands so that preheating leads to the front density decreasing rapidly, and consequently the Atwood number is reduced. Therefore, one needs to further discuss whether or not the modified Lindl formula can better predict the thick target behavior when there exists preheating. We postulate a thicker CH foil, with a thickness of 100 $\mu$m and a density of 1.0 g/cm$^3$. The pulse duration of a 0.53 $\mu$m laser is shaped in the following manner: a linear 3 ns ramp to an intensity of $3\times10^{14}$ W/cm$^2$, followed by an intensity that remains unchanged. At 5 ns, density perturbation with the wavelength 40 $\mu$m is superimposed on the one-dimensional density profile near the ablation front. The 2D simulation is performed in different adjusted $f(T)$ functions. Case 1: $f_1(T)$ is the same as $f(T)$. Case 2: $f_2(T)=1$, the Spitzer-Harm model with the limiter 0.05. Case 3: $f_3(T)=1$ is the same as the SH model when $T<43$ eV and when $T\geqslant172$ eV, but has a slight change when 43 eV$\leqslant T<172$ eV so as to show the SH effect on the RT growth rate. Case 4:

$$f_4(T)=\begin{cases}1.0, & T<8.6\ \text{eV}\\ 1500, & 8.6\ \text{eV}\leqslant T<17.2\ \text{eV}\\ 300, & 17.2\ \text{eV}\leqslant T<43\ \text{eV}\\ 2.5, & 43\ \text{eV}\leqslant T<86\ \text{eV}\\ 1.5, & 86\ \text{eV}\leqslant T<172\ \text{eV}\\ 1.0, & T\geqslant172\ \text{eV},\end{cases}$$

is chosen between both $f_3(T)$ and $f(T)$ for increasing preheating around the ablation front. Case 5: $f_5(T)=10/T^{3/2}$ (100 eV) when 1 eV$<T<$43 eV and $r>r_p-12$ $\mu$m so that the electron thermal conductivity versus $T$ generates a less sharp ablation front for considering the thermal transport of energetic electrons, where $r_p$ is the location of the peak density and the laser is incident on location $r_\infty$. Preheating at the head of the ablation front is less than 12 $\mu$m because the length of the preheated tongue is usually shorter than 12 $\mu$m. Case 6: $f_6(T)=3000/\rho$(g/cm$^3$) when 1 eV$<T<$43 eV and $r>r_p-12$ $\mu$m. This form $f(T)$ considers the fact that the mean free path of energetic electrons is inversely proportional to the mass density.

In Table I, $\gamma_c$, $\gamma_{cal}$, and $\gamma_{mT}$ are the RT growth rates for classic, two-dimensional simulation, and the modified Takabe formula, respectively. From Table I, we can see that the RT growth rates for cases 2 and 3 are greater than 80% of the classical value because of less preheating. However, as preheating increases from case 3 to case 4 and to case 1, the RT growth rate of the two-dimensional simulation decreases and the discrepancy increases between the value of the modified

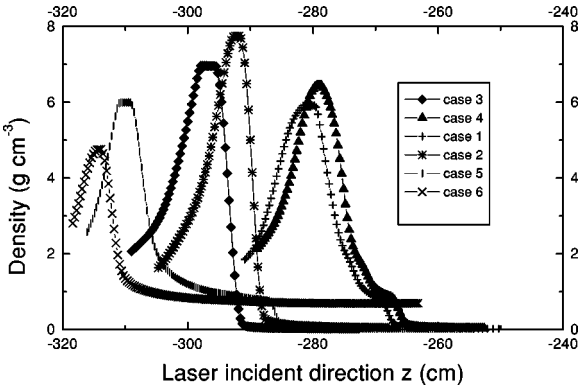


FIG. 2. The density profiles near the ablation front in different preheating cases.

Takabe formula and simulations. In the cases with more preheating, i.e., cases 5 and 6, similar results are shown. Particularly for case 6, the relative error of $\gamma_{cal}$ and $\gamma_{mT}$ is 26% though $L$ is smaller—only 2.27 $\mu$m.

Figure 2 shows the density profile of different preheating cases. For cases 2 and 3, $\rho_a$ is higher—over 7 g/cm$^3$—and $\rho_1$ is very low—about 0.2 g/cm$^3$, or below—so Atwood number $A$ is close to 1 in these two less preheating cases. However, for cases 1, 5, and 6, $\rho_a$ is lower, and $\rho_1$ increases to nearly 1 g/cm$^3$, so the Atwood number decreases to below 0.75. The density profiles of case 1 and case 5 are close; so are the Atwood numbers and the RT growth rates.

We see from the above results that even if a thick target is used in the preheating case, the modified Lindl formula (see Table I) given by $\gamma_{mL}$ still agrees very well with the results of our simulation (see $\gamma_{cal}$). The density profile near the ablation front is also distinctly changed and the Atwood number of the ablation front is clearly less than 1, so the Atwood number stabilization is important, This formula is reduced to the modified Takabe formula at $A=1$, and is closed to the Takabe formula at the steep ablation front.

In summary, the linear RT growth rate in our simulation agrees well with GL's experiment by enhancing the electron thermal conductivity at a lower temperature and higher density. In the ablation region, preheating not only reduces the peak density, but also raises the density at the foot of the ablation front, thus the Atwood number of the ablation front decreases and contributes to the reduction of the ablation RT growth rate. The modified Lindl formula $\gamma_{mL}=\sqrt{Akg/(1+AkL)}-2kV_a$ is better suited for the preheating case. It agrees well with the experiment value given by GL and our simulation. We believe that this stabilization effect is also important in the x-ray preheating case for the x-ray ablative RT instability.

We acknowledge helpful discussions with Dr. Shaoping Zhu. This work was supported by the National High-Tech ICF Committee, partly supported by the National Natural Science Foundation of China under Grant Nos. 19932010 and 10135010, and the National Basic Research Project ''Nonlinear Science'' in China.

[1] J. Lindl, Phys. Plasmas **2**, 3933 (1995).
[2] C.P. Verdon, Bull. Am. Phys. Soc. **38**, 2010 (1993).
[3] H. Takabe *et al.*, Phys. Fluids **28**, 3676 (1985).
[4] J. Sanz, Phys. Rev. Lett. **73**, 2700 (1994).
[5] S.G. Glendinning *et al.*, Phys. Rev. Lett. **78**, 3318 (1997).
[6] K. Shigemori *et al.*, Phys. Rev. Lett. **78**, 250 (1997).
[7] D.L. Tubbs *et al.*, Phys. Plasmas **6**, 2095 (1999).
[8] L. Spitzer and R. Harm, Phys. Rev. **89**, 977 (1953).
[9] M. Honda, Ph.D. thesis, Osaka University, 1998.
[10] P.L. Bhatnagar *et al.*, Phys. Rev. **94**, 511 (1954).
[11] R. Betti *et al.*, Phys. Plasmas **5**, 1446 (1998).
[12] H. Azechi *et al.*, Phys. Plasmas **4**, 4079 (1997).
[13] C.J. Pawley *et al.*, Phys. Plasmas **6**, 565 (1999).
[14] S.E. Bodner *et al.*, Phys. Plasmas **5**, 1901 (1998).
[15] Wenhua Ye *et al.*, High power Laser Parti Beams **10**, 403 (1998), in Chinese.
[16] J.P. Boris and D.L. Book, J. Comput. Phys. **11**, 38 (1973).
[17] A.R. Piriz *et al.*, Phys. Plasmas **1**, 1117 (1997).
[18] Yan Xu and X.T. He, Phys. Rev. E **50**, 443 (1994).
[19] E.P. Epperlein, Laser Part. Beams **12**, 257 (1994).
[20] M. Tabak *et al.*, Phys. Fluids B **2**, 1007 (1990).
[21] Y.T. Lee and R.M. More, Phys. Fluids **27**, 1273 (1984).